ACS APPLIED MATERIALS & INTERFACES

Research Article

Cite This: ACS Appl. Mater. Interfaces 2019, 11, 37434−37441

www.acsami.org

Patterned Photonic Array Based on an Intertwined Polymer Network Functionalized with a Nonenzymatic Moiety for the Visual Detection of Glucose

Sundas Munir, Saddam Hussain, and Soo-Young Park*

School of Applied Chemical Engineering, Polymeric Nano Materials Laboratory, Kyungpook National University, Daegu 41566, Republic of Korea

Supporting Information

ABSTRACT: A patterned photonic array chip based on an intertwined polymer network (IPN) is proposed for the visual detection of glucose. The IPN networks are composed of photonic and poly(acrylic acid) (PAA) networks. Aminophenylboronic acid, as a nonenzymatic glucose-responsive moiety that can covalently bond to glucose at alkaline pH, forming tetragonal complexes, is immobilized in the PAA network; in hydrogels, this bonding generates Donnan osmotic pressure, resulting in a volumetric increase of the photonic IPN and reflected color change. The photonic band gap wavelength linearly increases with the glucose concentration (in the 1−12 mM range), with a limit of detection of 0.35 mM. The dots of the photonic IPN array respond independently, with high sensitivity and stability, to glucose via color changes; different glucose levels, from hypo- to hyperglycemia, can be visually detected in this way. Serum samples spiked with different glucose concentrations were tested for practical evaluation of the chip. The proposed chip could be utilized as a new biosensor platform for cost-effective and easy visual detection in remote areas, without the need of advanced instruments or technology.

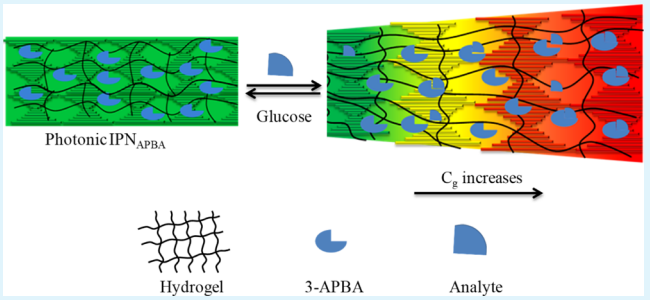

KEYWORDS: *array biosensors, glucose sensors, intertwined polymer networks, boronic acid−glucose interaction, Donnan osmotic pressure*

1. INTRODUCTION

Diabetes is one of the major health problems of the 21st century, with more than 420 million adults worldwide suffering from this metabolic disorder. It is estimated that one in three adults will be diagnosed with diabetes by 2050; its increasing incidence is causing significant economic costs, both directly because of the medical treatments required and indirectly by affecting the work of the patients. The maintenance of healthy blood glucose levels and minimized complications will benefit from accurate and continuous glucose monitoring systems. The demand for fast, reliable, and continuous measurements of the glucose levels in medicine, biotechnology, and environmental sciences has evolved into the need for small, easy-to-handle, and inexpensive analytical devices.[1,2]

Photonic crystals (PCs) have emerged as an attractive material for the development of optical sensors. Periodic alternation of refractive index in these materials allows them to reflect the light, observable in the visible region.[3] So far, several fabrication methods have been developed to fabricate responsive one-, two-, and three-dimensional PCs;[4] for example, stimuli-responsive PCs have received much interest in the last few decades for their possible applications in optical sensors.[5,6] Hydrogels with integrated photonic band gap structures have been optimized to undergo reversible changes in their physical dimensions in response to external stimuli such as glucose, pH, ionic strength, temperature, humidity, solvent composition, and biomolecule binding. The photonic band gaps of these sensors are sensitive to such a volumetric change, which is converted into readable optical information.

In the past, many photonic sensors (such as holographic, crystalline colloidal array, inverse opal, porous silicon, block copolymer, and Bragg stack sensors)[7] have been reported for the colorimetric detection of glucose; in these sensors, the hydrogel is either immobilized with glucose oxidase (GOx) or a nonenzymatic boronic acid receptor. For example, Holtz and Asher proposed a crystalline colloidal array of polymer spheres within an acrylamide hydrogel functionalized with GOx, which swells according to different glucose concentrations.[8] Elsherif et al. have achieved glucose sensing by using phenylboronic acid-functionalized hydrogel-based optical diffusers, which alter the diffusion spectra and transmitted beam profile by the volumetric expansion of the hydrogel upon binding with glucose;[9] similarly, Hong et al. used self-assembled PC microspheres polymerized with comonomers of methyl

Received: June 12, 2019
Accepted: September 23, 2019
Published: September 23, 2019

DOI: 10.1021/acsami.9b10316
ACS Appl. Mater. Interfaces 2019, 11, 37434−37441

Scheme 1. Fabrication Procedure for the Photonic IPN-Based Array Sensor

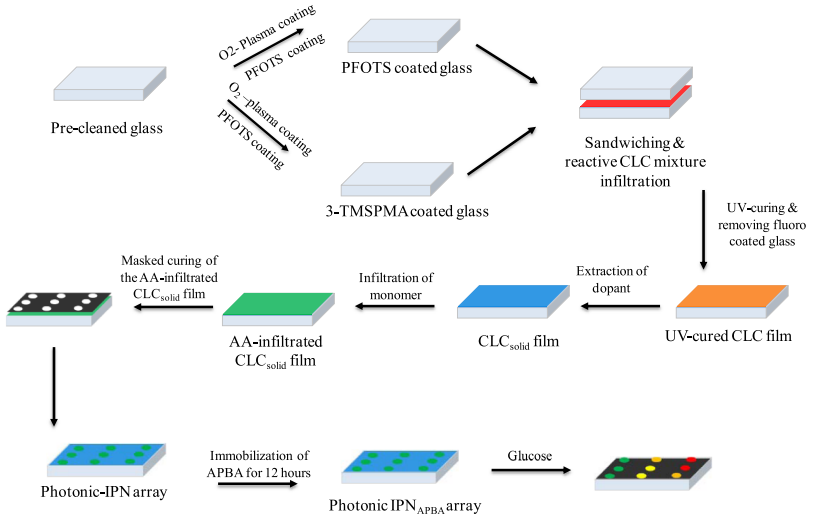

methacrylate, *N*-isopropylacrylamide, and 3-acrylamidophenylboronic.[10] Guan et al. have reported the fabrication of a glucose sensor, in which the responsive crystalline colloidal array (CCA) of poly(*N*-isopropylacrylamide-*co*-3-acrylamidophenylboronic acid) [P(NIPAA$_m$-*co*-AA$_m$PBA)] microgel particles was incorporated in the nonresponsive hydrogel matrix of poly(AA$_m$).[11] Upon binding with glucose, only photonic intensity changed without shift of the wavelength at photonic band gap (λ_{PBG}). Zhang et al. have reported the utilization of an ultrathin hydrogel film prepared by layer-by-layer assembly of poly(vinyl alcohol)/poly(AA$_m$-*co*-AA$_m$PBA) with thickness on a sub-micrometer scale for the detection of glucose with short response time.[12] The hydrogel films responded to the variations in glucose concentration, via the shift of Fabry−Perot fringes. In another report, they also reported the interlocked photonic poly(NIPAA$_m$) microgel particles having polymerizable vinyl groups on the surface.[13] The resulting interlocked photonic CCA (PCCA) responded to both temperature and salt, and the λ_{PBG} could be tuned in a wide range of visible spectra. Zhang et al. have reported a PCC film of poly(NIPAA$_m$) microgel particles doped with P(NIPAA$_m$-*co*-AA$_m$PBA) as a glucose sensor, which exploits a structural order−disorder transition, instead of change in lattice constant, upon binding with glucose.[14] As the concentation of the aqueous glucose solution (C_g) changes, a change in the intensity at the λ_{PBG} is observed. All these sensors allow the detection of different glucose concentrations, semiquantitatively by eye or quantitatively by spectrophotometer. However, their glucose-responding PC structures need complex, tedious, and delicate preparation methods. Thus, new cost-effective, easy-to-make, and stable PC structures having an array form are highly desirable.

Low-molecular-weight reactive cholesteric liquid crystals (CLCs) have been recently used for fabricating one-dimensional PCs; their helicoidal structure is fixed via ultraviolet (UV)-curing to obtain complete solid-state CLCs (CLC$_{solid}$). They are usually prepared by mixing reactive mesogens with a chiral dopant. Their helical pitch can be controlled by the amount of chiral dopant so as to obtain a structure having the λ_{PBG} that matches the wavelength of visible light. The removal of the unreacted chiral dopant can create spaces in solid-state one-dimensional photonic structures,[15] which can be used to infiltrate functional materials for biosensing. Hydrogels are smart materials able to change their properties, with an isotropic increase or decrease in volume, in response to the external stimuli.[16] The combination of hydrogels and CLCs results in photonic intertwined polymer networks (IPNs),[17] which combine the responsive isotropic properties of the former with the anisotropic and helicoidal molecular order of the latter. The pH and humidity responsiveness of such photonic IPNs has already been studied;[18] their application for biosensing purposes requires selectivity, which could be introduced by immobilizing different molecular recognition groups such as enzymes, antibodies, and aptamers;[19−22] however, the enzyme-based technology is limited by the generation of H_2O_2 (strong oxidizing agent), high costs, and critical operating conditions.[23] Phenylboronic acid-functionalized hydrogels can be an alternative solution to obtain such selectivity because of their affinity to glucose molecules. Different derivatives of boronic acid (BA) receptors bond covalently and reversibly with the diol moieties of glucose and various boronate complexes (trigonal/tetragonal) could form depending on the medium's pH. The complexation between aminophenylboronic acid (APBA) and glucose generates Donnan osmotic pressure, resulting in such volumetric changes that the hydrogel swells to different extents according to the analyte concentration;[24] in addition, this volumetric change simultaneously alters the pitch and color of the light reflected by the photonic IPN.

In this study, we developed a glucose array sensor via the selective curing of the photonic IPN film, by photolithography, and its subsequent immobilization with APBA via 1-ethyl-3-(3-dimethylaminopropyl)carbodiimide (EDC) coupling (Scheme 1). Photonic dots respond to the presence of glucose by changing their color depending upon the concentration, with high stability (owing to its solid-state structure), specificity (given by the immobilization of the glucose recognition group), and sensitivity. Therefore, the proposed array sensor could allow the screening of different levels of glucose by the naked eye, with no need for sophisticated analytical instruments and electrical components.

2. EXPERIMENTAL SECTION

2.1. Materials. A reactive liquid crystal mixture (RMM727; Merck, UK); (*S*)-4-cyano-4′-(2-methylbutyl) biphenyl (CB15; Synthon, Germany); acrylic acid (AA; Junsei, Japan); Irgacure 500 (Ciba

DOI: 10.1021/acsami.9b10316
ACS Appl. Mater. Interfaces 2019, 11, 37434−37441

Inc., Switzerland); APBA (Sylgard 184; Dow Corning, USA); tripropylene glycol diacrylate (TPGDA), 3-(trimethoxysilyl)propyl methacrylate (TMSPMA) (98%), trichloro(1*H*,1*H*,2*H*,2*H*-perfluorooctyl)silane (PFOTS, 97%),*N*-hydroxysuccinimide (NHS), *N*-(3-dimethylaminopropyl)-*N*′-ethylcarbodiimide HCl(EDC·HCl), octadecyltrichlorosilane (OTS), glucose, and human serum from Sigma-Aldrich (USA); micro-pearl (Sekisui, Japan); acetone, ethanol, and phosphate-buffered saline (PBS) from Duksan (Republic of Korea) were all used as received. Deionized (DI) water, used for all experiments unless otherwise mentioned, was purified using a reverse-osmosis system (μPure RO; Romax, Republic of Korea). Optimized amounts of RMM727 and CB15 (26 wt %) were mixed at 85 °C for 30 min under continuous magnetic stirring; after complete stirring and cooling to 25 °C, the transparent chiral mixture solution turns milky.

2.2. Glass Functionalization. The glass substrates were cleaned by sonication in ethanol for 15 min, followed by washing with DI water and drying under air pressure. The TMSPMA solution was spin-coated (at 3000 rpm for 45 s) onto their activated surface, previously prepared using O_2 plasma. After curing at 100 °C for 10 min, these substrates were ready to use. The PFOTS was also coated onto the other glass surface via chemical vapor deposition in a closed chamber, at 70 °C for 1 h.

2.3. Formation of the CLC Film. The CLC mixture (20 μL) was allowed to infiltrate between the two TMSPMA- and PFOTS-sandwiched glasses, separated by a 6 μm thick spacer. After infiltration, this mixture was photopolymerized at 365 nm and 20 °C for 10 min by using a UV-curing machine (Innocure 100N; Lichtzen, Republic of Korea). The unreacted CB15 was removed by washing with acetone repeatedly. Various techniques confirmed both the formation of the photonic structure and the removal of unreacted CB15.

2.4. Preparation of the Photonic IPN Array Dots. The monomer mixture (AA/TPGDA/Irgacure 500, 98.5:0.5:1 wt %)[25] was dropped onto the CLC film and allowed to infiltrate for 30 min, after which no visible color change was observed and its excess was removed before the UV-curing. Then, the film was selectively photopolymerized for 10 min by using a photomask placed at 6 cm from it. Next, different APBA concentrations were immobilized on the individual dots, followed by EDC·HCl/NHS (1:2 molar ratio, pH = 7) coupling for 2 h and drying in air. The APBA immobilization was confirmed through FTIR spectroscopy. The prepared IPN with APBA immobilization is denoted as IPN_{APBA}. The color change of the photonic IPN_{APBA} dots in response to different C_g was recorded. All aqueous glucose solutions were prepared in carbonate buffer, pH = 8.5.

2.5. Characterization. Cross-sectional images of the photonic IPN array were obtained using a field-emission scanning electron microscope (SEM; SU8220; Hitachi, Japan) operated at 15 kV; the samples were prepared by coating their surfaces with platinum. Attenuated total reflection Fourier-transform infrared (FTIR) spectra were obtained with an FTIR spectrometer (FT/IR-4100; Jasco, Japan) in the 600−4000 cm^{-1} range at a resolution of 4 cm^{-1} by collecting an average of 64 scans. UV−vis spectra of the CLC films in the 300−900 nm range were obtained using a bench-top UV spectrophotometer (Ocean Optics, DH-2000-BAL); the films were oriented perpendicularly to the beam.

3. RESULTS AND DISCUSSION

To obtain a sequential IPN-based patterned array, the reactive CLC mixture was infiltrated by capillary force in the gap between two glass plates (an upper PFOTS-coated and a bottom TMSPMA-coated one), resulting in a red reflection band at λ_{PBG} = 650 nm (Figures S1a and 1); λ_{PBG} is the wavelength at photonic band gap measured from the peak of the UV−vis spectrum. After photopolymerization, the resultant UV-cured CLC film (Figure S1b) exhibited an orange/red reflection band at λ_{PBG} = 615 nm (Figure 1); its FTIR

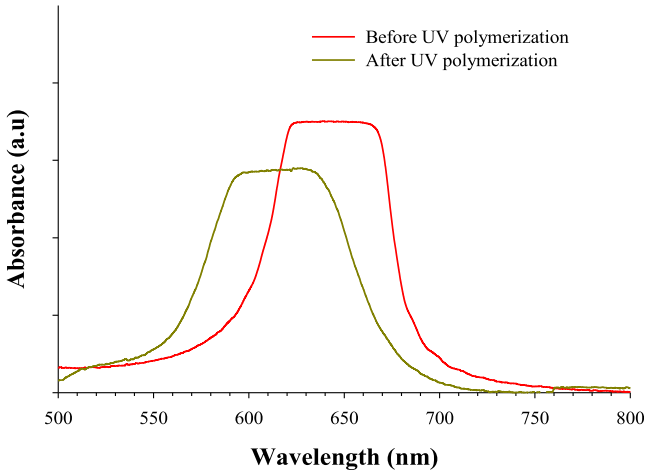

Figure 1. UV−vis spectra of the reactive CLC film, before and after UV polymerization.

spectrum confirmed the absence of the characteristic acrylate peaks (C═C) at 1635 and 810 cm^{-1}, suggesting that the acrylate double bonds in the used reactive mesogen mixture of RMM727 were polymerized by the UV irradiation (Figure S2a).

The upper PFOTS-coated glass was removed after the photopolymerization, leaving the UV-cured CLC film on the bottom 3-TMSPMA-coated glass. Then, after washing 10 times with acetone to extract CB15, the resulting CLC_{solid} film showed a blue color at the reflection band at λ_{PBG} = 460 nm, revealing that its photonic structure was preserved with the decreased helical pitch (Figure 2a,d). The CB15 removal was further confirmed by FTIR analysis; the characteristic peak of

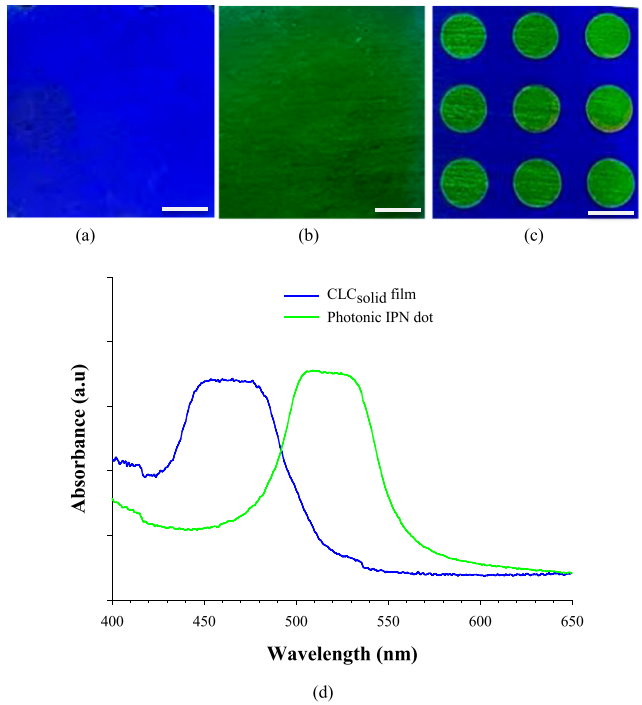

Figure 2. Photographs of the (a) CLC_{solid} film, (b) AA-infiltrated CLC_{solid} film, and the (c) photonic IPN array film. (d) UV−vis spectra of the CLC_{solid} film and the photonic IPN dots. Scale bar for all the images is 2 mm.

DOI: 10.1021/acsami.9b10316
ACS Appl. Mater. Interfaces 2019, 11, 37434−37441

the cyano group at 2220 cm^{-1} almost disappeared (Figure S2b). The removal of the CB15 may provide easy access to other molecules into the CLC_{solid} matrix.

The infiltration of the AA−TPGDA mixture into the CLC_{solid} film resulted in a color change from blue to green, revealing the film swelling because of the infiltrated AA monomers (Figure 2b); the green color saturated 20 min after this addition. When the infiltration was completed, the AA-infiltrated CLC_{solid} film was selectively photopolymerized and the unreacted AA monomers outside the dot areas were washed away by using a PBS solution (pH = 7). The so-obtained photonic IPN array exhibited a green reflection (λ_{PBG} = 520 nm) at the dot areas and a blue one (λ_{PBG} = 460 nm) around them. The FTIR spectra of the dot areas showed peaks at 3500, 3000, 1750, and 1408 cm^{-1} that were attributed to, the non-hydrogen-bonded −OH stretching of the carboxylic acid group, NH stretches, symmetric and asymmetric stretching bands of the carboxylic acid group, and carboxylate ions, respectively (Figure S2c). These results, therefore, demonstrate the successful formation of a poly(acrylic acid) (PAA) network in these photonic dots.

Figure 3a displays a cross-sectional SEM image of the CLC_{solid} film, showing periodically alternating dark and bright

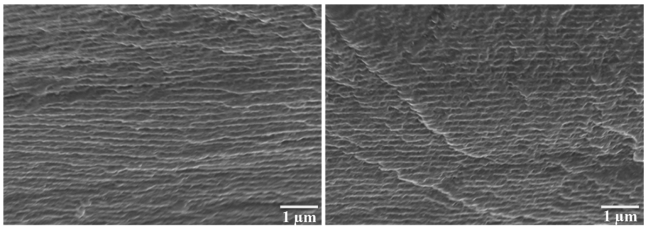

(a) (b)

Figure 3. Cross-sectional SEM images of the (a) CLC_{solid} and (b) photonic IPN films.

layers that reveal the formation of a solid-state photonic structure; this periodicity (245 nm) represents $p/2$, where p is the helix pitch. Figure 3b shows a cross-sectional SEM image of the photonic IPN film, revealing an increased periodicity (260 nm) because of the infiltrated network. The λ_{PBG} was calculated by $p \times n$, where n is the refractive index, and its values for the CLC_{solid} and photonic IPN films were 460 and 520 nm, respectively, which are well matched with the corresponding observed colors (blue and green).

For glucose detection, the photonic IPN dots were activated using EDC·HCl/NHS (molar ratio 2:1) as a coupling agent for APBA. APBA in different concentrations (C_{APBA}) was immobilized on the individual IPN_{APBA} dots to find its optimum amount. The FTIR spectra of these dots showed peaks at 1253, 1555, 1631, 1708, and 3400 cm^{-1}, which were attributed to, respectively, the B−OH stretching vibrations, the $C{=}C_{aromatic}$ vibrations, the amide-I formation, and the C=O and $-OH/NH_2$ stretching of the covalently immobilized APBA (Figure S2d).

When a photonic IPN_{APBA} forms tetragonal complexes with glucose at alkaline pH, Donnan osmotic pressure is generated, resulting in volumetric changes of the matrix (Scheme 2). Figure S3 shows the side view of 5 × 5 photonic IPN arrays after immobilizing APBA with different C_{APBA}. The aqueous glucose solution was contained in the IPN dot areas, forming drops without cross-contamination because of the hydrophilic and hydrophobic natures of the dot and background areas,

Scheme 2. Glucose Binding with APBA, Which Causes the Swelling of the Photonic IPN Dots Immobilized with APBA

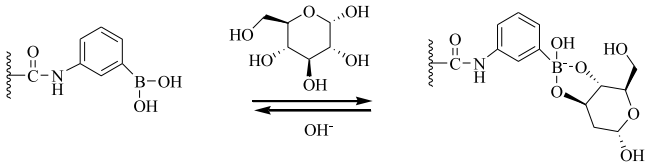

respectively. Figure 4 shows the photographic image of the photonic IPN_{APBA} array immersed in a 5 mM glucose solution,

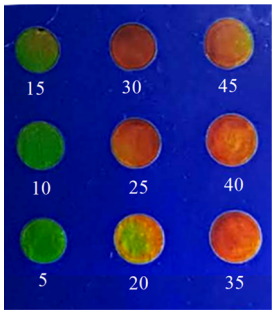

Figure 4. Photograph of a 3 × 3 APBA-immobilized photonic IPN array immersed in a 5 mM glucose solution (the numbers represent the APBA concentration in mM).

and the UV−vis spectra of its dot areas are displayed in Figure S4. In the cases of low C_{APBA} (5−10 mM), the initial green color of the dots was maintained although λ_{PBG} was slightly red-shifted from 520 (without glucose) to 534 nm. When C_{APBA} increased to 15 mM, a slight yellow color arose (568 nm). As C_{APBA} further increased to 20 and 25 nm, yellow-orange (593 nm) and red (607 nm) colors were respectively seen. At C_{APBA} = 30 mM, red color was clearly observed (645 nm) and saturated with further C_{APBA} increase. Thus, the aqueous solution with 30 mM APBA was selected for the next sensing tests. Three dots of the IPN array film without immobilization of APBA were tested with 2, 5, and 10 mM glucose aqueous solutions. Figure S5 shows their photographic images. Its initial green color was maintained after glucose solution was dropped on the dot, indicating that the photonic color change of the IPN_{APBA} array dot is caused by swelling of the hydrogel in the photonic IPN_{APBA} through Donnan osmotic pressure, which occurs by the complex formation between APBA and glucose.

Asher et al. studied the PCCA incorporated into a polyacrylamide hydrogel with pendent BA groups.[26] The embedded CCA diffracts visible light, and the diffraction wavelength of PCCA reports on the hydrogel volume. The BA in PCCA responds to species containing vicinal cis diols such as carbohydrates. This PCCA responds to glucose at low ionic strength by swelling of PCCA and red-shifting of the λ_{PBG} as the C_g increases. The hydrogel swelling results from a Donnan potential because of formation of boronate anion. This sensing material responds to glucose and other sugars at <50 μM concentrations in low-ionic-strength solutions. Asher et al. also developed a PCCA system working at high ionic strength.[27] They utilized the CCA embedded into the $BA-AA_m-$polyethylene glycol (PEG) hydrogel to detect glucose with NaCl salts at physiological salinities (high ionic strength). They utilized $PEG-Na^+$ to form a bis-bidentate complex between glucose and two boronates. The formation of the

DOI: 10.1021/acsami.9b10316
ACS Appl. Mater. Interfaces 2019, 11, 37434−37441

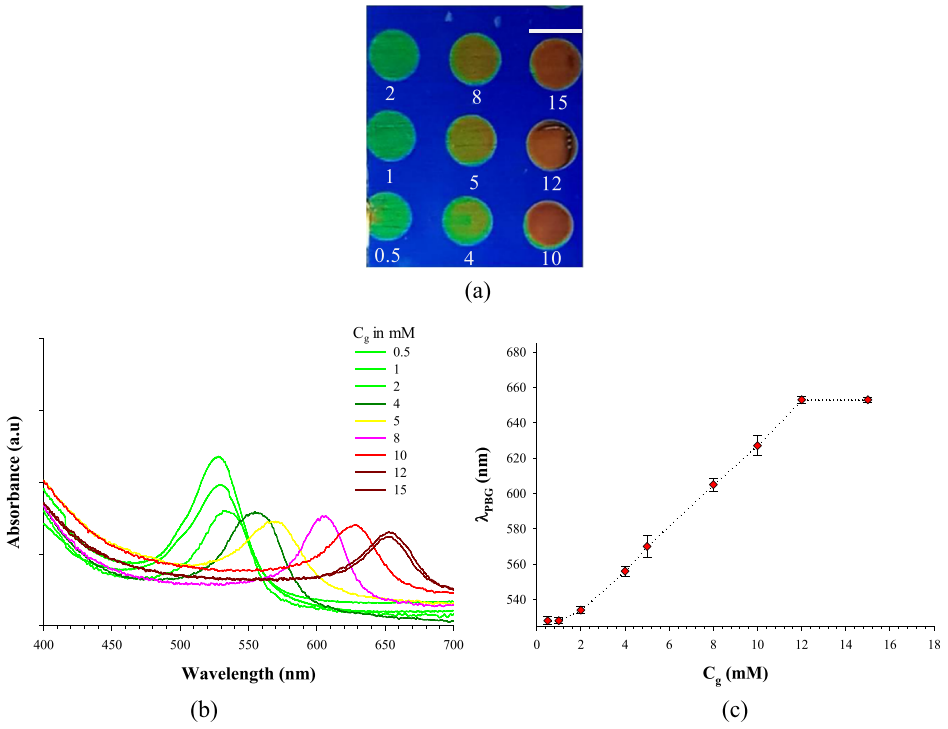

Figure 5. (a) Photographic image in reflection mode of a 3 × 3 photonic IPN_{APBA} array, (b) UV−vis spectra of its dots at different glucose concentrations (C_g), and (c) wavelength at photonic band gap (λ_{PBG}) as a function of C_g; the numbers in (a) indicate the C_g values in mM and the error bars in (c) represent the mean ± standard deviation for three time measurements.

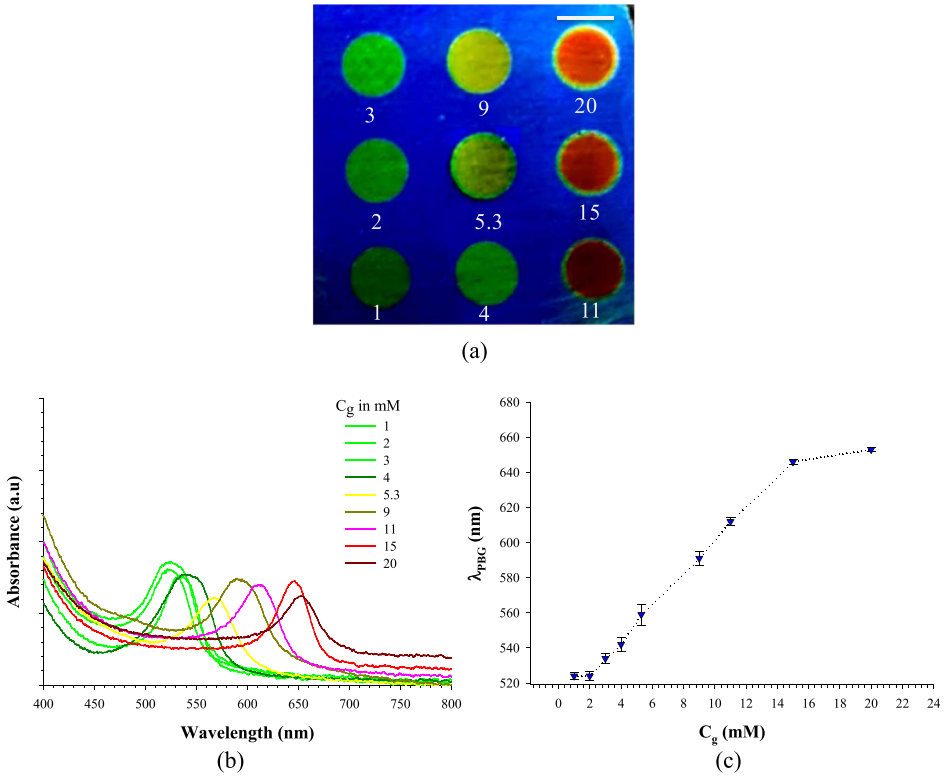

Figure 6. (a) Photographic image in reflection mode of a 3 × 3 photonic IPN_{APBA} array, (b) UV−vis spectra of its dots at different glucose concentrations (C_g) in human serum, and (c) wavelength at photonic band gap (λ_{PBG}) as a function of C_g; the numbers in (a) indicate the C_g values in mM and the error bars in (c) represent the mean ± standard deviation for three times.

complex results in an increase in the hydrogel cross-linking and leads to the blue shift of the λ_{PBG} upon binding with glucose. There was no change in the λ_{PBG} without PEG, and it red-shifted without NaCl salts in their system. In our case, PEG and salts were not used so that the reversible bonding of glucose to boronate ions at alkaline pH gives rise to a Donnan

DOI: 10.1021/acsami.9b10316
ACS Appl. Mater. Interfaces 2019, 11, 37434−37441

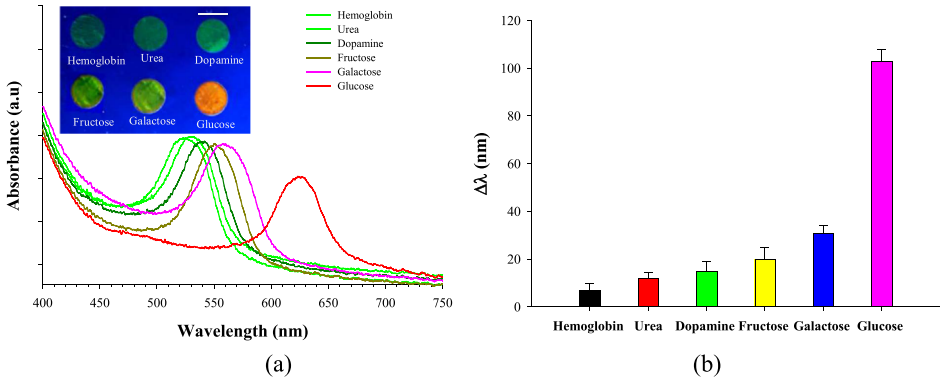

Figure 7. (a) UV−vis spectra of a 2 × 3 photonic IPN_{APBA} array together with (inset) its photographic image in reflection mode and (b) the resulting wavelength difference at the photonic band gap ($\Delta\lambda$) as a function of the glucose concentration, after exposure to 0.01 M solutions of different blood interferents (hemoglobin, urea, dopamine, fructose, galactose, and glucose); the error bars in (b) indicate the mean ± standard deviation for measurements three times.

potential by which an osmotic pressure (and swelling of the hydrogel) is generated.

3.1. Sensitivity of the Photonic IPN_{APBA} Array. A blank test was performed by dropping an aqueous solution (0 mM, pH = 8.5) on the dots of the IPN_{APBA} array as shown in Figure S6. The dots do not show any variation in its green color. This result demonstrates that the swelling of dots is owing to binding of glucose with IPN_{APBA}. Figure 5 shows the photographic images, UV−vis spectra, and λ_{PBG} plot of the photonic IPN_{APBA} dots for different glucose concentrations (C_g). For C_g = 0.5 mM (hypoglycemic level), the dots retained in the initial green color although a little red shift from 520 (without glucose) to 526 nm was observed. As C_g increased to 2 and 5 mM (hypoglycemic and normal levels, respectively), emerald green (534 nm) and yellow (570 nm) colors were correspondingly seen. At C_g = 5.2−6.8 and 9 mM (normal and hyperglycemic levels, respectively), orange-red (590 nm) and red (627 nm) colors correspondingly arose. At C_g > 10 mM (diabetic range), λ_{PBG} reached 653 nm and saturated. Thus, the fabricated array chip could simultaneously use nine dots which individually work with different glucose concentrations via visual detection within the responsive glucose-concentration range.

The limit of detection (LOD) and linear range was obtained from the plot (Figure 5C). The LOD was calculated by using LOD = 3.3 × (SD/s) where SD is the standard deviation of a blank sample and s is the slope of the graph.[28] The calculated LOD was 0.35 mM with a linear range of 1−12 mM. Therefore, the proposed photonic IPN_{APBA} array chip can detect glucose, qualitatively via visual color change and quantitatively via the λ_{PBG} value. The response time of the photonic IPN_{APBA} array was studied. Figure S7 shows the photographic image of the photonic IPN_{APBA} array after the glucose solution (10 mM, 4 μL) was dropped on the dot. The green dot was changed to the red one within 12 min. It is a little longer than the response time (0.48 min) of the sensors prepared by Zhang et al.[29] although it is fast enough to apply biosensors.

3.2. Selectivity of the Photonic IPN_{APBA} Array in a Serum. For the practical application in glucose biosensors, the photonic IPN_{APBA} array was tested on human serum. The initial C_g value in the reference sample, measured via high-performance liquid chromatography, was 5.32 mM.[30] Hypoglycemic and hyperglycemic samples were prepared by diluting this human serum with carbonate buffer (pH = 8.5) and adding glucose to get the various C_g values desired. Figure 6 shows the photographic images, UV−vis spectra, and λ_{PBG} plot of the photonic IPN_{APBA} dots for serum samples with different C_g. A green-to-red color change was observed as C_g in the human serum sample increases. The initial green color (526 nm) at C_g = 0.5 mM became emerald green at 2 mM, yellow at 5 mM, orange-red at 5.2−6.8 mM, and red above 9 mM. The linear range and LOD derived from the λ_{PBG} versus C_g plot (Figure 5c) were 1−12 and 0.35 mM, respectively, which are similar to those derived from Figure 6; hence, the different glucose levels, ranging from hypoglycemic to diabetic ranges, could be quantitatively characterized. The glucose level was measured independently with a commercially available instrument (FUJI DRI-CHEM NX500, Japan). Table S1 shows the controlled and measured glucose levels. The glucose level was controlled by diluting serum with DI water or adding more glucose to the serum. The measured values are in close agreement with the controlled ones. The prepared sensors were able to detect glucose in human serum samples with almost the same sensitivity as that previously observed in aqueous solutions.

The selectivity of the photonic IPN_{APBA} array chip was tested against the major blood interferents such as hemoglobin, urea, dopamine, fructose, and galactose. Figure 7 shows the photographic images, UV−vis spectra, and λ_{PGB} difference ($\Delta\lambda$) plot after dropping the analyte solutions on the dots; in all cases, the absorption band was slightly red-shifted to different extents. The $\Delta\lambda_{PBG}$ values for hemoglobin, urea, and dopamine were 7, 12, and 15 nm, respectively; sugars like fructose and galactose resulted in bigger $\Delta\lambda$ (20 and 31 nm, respectively) because of their structural similarity with the glucose molecule. Glucose induced the highest $\Delta\lambda_{PBG}$ (103 nm), yielding a red color. The effects of charge interactions of metal ions (ionic strength) with the IPN_{APBA} array were studied as shown in Figure S8. The physiological concentrations of Ca^{2+}, Mg^{2+}, K^+, and Na^+ ions in blood are 2.2−2.8, 0.8−1.2, 3.5−5, and 136−145 mM, respectively.[31,32] The dots retain their initial green color after the treatment of metal ions at physiological concentrations, indicating that the ionic strength at physiological concentrations does not affect the photonic response of the IPN_{APBA} array. The strength of BA binding to saccharides is determined by the orientation and relative position of hydroxyl groups.[33] BA can differentiate structurally similar saccharide molecules. Monoboronic acids are known to exhibit inherent selectivity toward fructose over

DOI: 10.1021/acsami.9b10316
ACS Appl. Mater. Interfaces 2019, 11, 37434−37441

other monosaccharides. This is because fructose contains a syn-periplanar pair of hydroxyl groups available for BA binding. The binding selectivity for glucose is known to be much improved by using properly positioned multiboronic acids like our system. Remarkable progress has been made for developing BA-based sensors selective for glucose by following a general concept that suitably arranged multiple BA groups that favor multivalent saccharides.[24] Thus, the photonic IPN_{APBA} array could detect glucose against the major blood interferents with high selectivity.

4. CONCLUSIONS

A photonic IPN_{APBA} array consisting of a CLC_{solid} film and a PAA network was successfully fabricated by selective UV-curing with a photomask and APBA immobilization in the hydrogel polymer network. The so-obtained array chip allowed the detection of the hypo- and hyperglycemic ranges, both qualitatively by visual observation of its color change and quantitatively by analyzing it with a spectrophotometer, without any cross-contamination among the array dots; moreover, it exhibited excellent selectivity in real human serum samples. Thus, the proposed photonic IPN_{APBA} array could be used as a new array sensor for the easy visual detection of the glucose levels, with no need for sophisticated instruments in remote areas without the need of electrical components.

■ ASSOCIATED CONTENT

Supporting Information

The Supporting Information is available free of charge on the ACS Publications website at DOI: 10.1021/acsami.9b10316.

Photographic images, FTIR spectra, and UV−visible spectra (PDF)

■ AUTHOR INFORMATION

Corresponding Author

*E-mail: psy@knu.ac.kr. Phone: +82 10 9608 5630. Fax: +82 53 950 6623.

ORCID

Soo-Young Park: 0000-0001-6796-4929

Notes

The authors declare no competing financial interest.

■ ACKNOWLEDGMENTS

This work was supported by the South Korean National Research Foundation (2017R1A2B2006818).

■ ABBREVIATIONS

IPN, intertwined polymer network
PAA, poly acrylic acid
APBA, aminophenylboronic acid
PBG, photonic band gap
CLCs, cholesteric liquid crystals
EDC, 1-ethyl-3-(3-dimethylaminopropyl)carbodiimide
PFOTS, trichloro(1*H*,1*H*,2*H*,2*H*-perfluorooctyl)silane
TMSPMA, 3-(trimethoxysilyl)propyl methacrylate
OTS, octadecyltrichlorosilane
LOD, limit of detection

■ REFERENCES

(1) Albayrak, D.; Karakuş, E. A Novel Glutamine Biosensor Based on Zinc Oxide Nanorod and Glutaminase Enzyme from Hypocria Jecorina. *Artif. Cells, Nanomed., Biotechnol.* **2016**, *44*, 92−97.

(2) Sharma, B.; Bugga, P.; Madison, L. R.; Henry, A.-I.; Blaber, M. G.; Greeneltch, N. G.; Chiang, N.; Mrksich, M.; Schatz, G. C.; Van Duyne, R. P. Bisboronic Acids for Selective, Physiologically Relevant Direct Glucose Sensing with Surface-Enhanced Raman Spectroscopy. *J. Am. Chem. Soc.* **2016**, *138*, 13952−13959.

(3) Ho, K. M.; Chan, C. T.; Soukoulis, C. M. Existence of a Photonic Gap in Periodic Dielectric Structures. *Phys. Rev. Lett.* **1990**, *65*, 3152−3155.

(4) Xu, Y.; Zhou, G.; Zhu, D. Three New Organically Templated 1D, 2D, and 3D Vanadates: Synthesis, Crystal Structures, and Characterizations. *Inorg. Chem.* **2008**, *47*, 567−571.

(5) Inan, H.; Poyraz, M.; Inci, F.; Lifson, M. A.; Baday, M.; Cunningham, B. T.; Demirci, U. Photonic Crystals: Emerging Biosensors and their Promise for Point-of-Care Applications. *Chem. Soc. Rev.* **2017**, *46*, 366−388.

(6) Shirazi, M.; Jeon, M.; Kim, J. Structural Analysis of Polymer Composites Using Spectral Domain Optical Coherence Tomography. *Sensors* **2017**, *17*, 1155.

(7) Yetisen, A. K.; Butt, H.; Volpatti, L. R.; Pavlichenko, I.; Humar, M.; Kwok, S. J. J.; Koo, H.; Kim, K. S.; Naydenova, I.; Khademhosseini, A.; Hahn, S. K.; Yun, S. H. Photonic Hydrogel Sensors. *Biotechnol. Adv.* **2016**, *34*, 250−271.

(8) Holtz, J. H.; Asher, S. A. Polymerized Colloidal Crystal Hydrogel Films as Intelligent Chemical Sensing Materials. *Nature* **1997**, *389*, 829−832.

(9) Elsherif, M.; Hassan, M. U.; Yetisen, A. K.; Butt, H. Glucose Sensing with Phenylboronic Acid Functionalized Hydrogel-Based Optical Diffusers. *ACS Nano* **2018**, *12*, 2283−2291.

(10) Hong, X.; Peng, Y.; Bai, J.; Ning, B.; Liu, Y.; Zhou, Z.; Gao, Z. A Novel Opal Closest-Packing Photonic Crystal for Naked-Eye Glucose Detection. *Small* **2014**, *10*, 1308−1313.

(11) Liu, Y.; Zhang, Y.; Guan, Y. New Polymerized Crystalline Colloidal Array for Glucose Sensing. *Chem. Commun.* **2009**, 1867−1869.

(12) Zhang, X.; Guan, Y.; Zhang, Y. Ultrathin Hydrogel Films for Rapid Optical Biosensing. *Biomacromolecules* **2011**, *13*, 92−97.

(13) Chen, M.; Zhou, L.; Guan, Y.; Zhang, Y. Polymerized Microgel Colloidal Crystals: Photonic Hydrogels with Tunable Band Gaps and Fast Response Rates. *Angew. Chem., Int. Ed.* **2013**, *52*, 9961−9965.

(14) Jia, S.; Tang, Z.; Guan, Y.; Zhang, Y. Order−Disorder Transition in Doped Microgel Colloidal Crystals and Its Application for Optical Sensing. *ACS Appl. Mater. Interfaces* **2018**, *10*, 14254−14258.

(15) Mulder, D. J.; Schenning, A. P. H. J.; Bastiaansen, C. W. M. Chiral-Nematic Liquid Crystals as one Dimensional Photonic Materials in Optical Sensors. *J. Mater. Chem. C* **2014**, *2*, 6695−6705.

(16) Ji, F.; Yong, Z.; JinLian, H.; Yan, L.; Lap-Yan, Y.; GuangDou, Y. Smart Polymer Fibers with Shape Memory Effect. *Smart Mater. Struct.* **2006**, *15*, 1547.

(17) Myung, D.; Waters, D.; Wiseman, M.; Duhamel, P.-E.; Noolandi, J.; Ta, C. N.; Frank, C. W. Progress in the Development of Interpenetrating Polymer Network Hydrogels. *Polym. Adv. Technol.* **2008**, *19*, 647−657.

(18) Stumpel, J. E.; Gil, E. R.; Spoelstra, A. B.; Bastiaansen, C. W. M.; Broer, D. J.; Schenning, A. P. H. J. Stimuli-Responsive Materials Based on Interpenetrating Polymer Liquid Crystal Hydrogels. *Adv. Funct. Mater.* **2015**, *25*, 3314−3320.

(19) Munir, S.; Kang, I.-K.; Park, S.-Y. Polyelectrolytes Functionalized Nematic Liquid Crystal-Based Biosensors: an Overview. *Trac. Trends Anal. Chem.* **2016**, *83*, 80−94.

(20) Khan, M.; Park, S.-Y. Liquid Crystal-Based Proton Sensitive Glucose Biosensor. *Anal. Chem.* **2014**, *86*, 1493−1501.

(21) Khan, M.; Park, S.-Y. Specific Detection of Avidin−Biotin Binding Using Liquid Crystal Droplets. *Colloids Surf., B* **2015**, *127*, 241−246.

DOI: 10.1021/acsami.9b10316
ACS Appl. Mater. Interfaces 2019, 11, 37434−37441

(22) Zhou, W.; Jimmy Huang, P.-J.; Ding, J.; Liu, J. Aptamer-Based Biosensors for Biomedical Diagnostics. *Analyst* **2014**, *139*, 2627−2640.
(23) Mani, S.; Vediyappan, V.; Chen, S.-M.; Madhu, R.; Pitchaimani, V.; Chang, J.-Y.; Liu, S.-B. Hydrothermal Synthesis of Niwo4 Crystals for High Performance Non-Enzymatic Glucose Biosensors. *Sci. Rep.* **2016**, *6*, 24128.
(24) Wu, X.; Li, Z.; Chen, X.-X.; Fossey, J. S.; James, T. D.; Jiang, Y.-B. Selective Sensing of Saccharides Using Simple Boronic Acids and their Aggregates. *Chem. Soc. Rev.* **2013**, *42*, 8032−8048.
(25) Noh, K.-G.; Park, S.-Y. Biosensor Array of Interpenetrating Polymer Network with Photonic Film Templated from Reactive Cholesteric Liquid Crystal and Enzyme-Immobilized Hydrogel Polymer. *Adv. Funct. Mater.* **2018**, *28*, 1707562.
(26) Asher, S. A.; Alexeev, V. L.; Goponenko, A. V.; Sharma, A. C.; Lednev, I. K.; Wilcox, C. S.; Finegold, D. N. Photonic Crystal Carbohydrate Sensors: Low Ionic Strength Sugar Sensing. *J. Am. Chem. Soc.* **2003**, *125*, 3322−3329.
(27) Alexeev, V. L.; Sharma, A. C.; Goponenko, A. V.; Das, S.; Lednev, I. K.; Wilcox, C. S.; Finegold, D. N.; Asher, S. A. High Ionic Strength Glucose-Sensing Photonic Crystal. *Anal. Chem.* **2003**, *75*, 2316−2323.
(28) Cho, M.-J.; Park, S.-Y. Carbon-Dot-Based Ratiometric Fluorescence Glucose Biosensor. *Sens. Actuators, B* **2019**, *282*, 719−729.
(29) Li, Q.; Guan, Y.; Zhang, Y. Thin Hydrogel Films Based on Lectin-Saccharide Biospecific Interaction for Label-Free Optical Glucose Sensing. *Sens. Actuators, B* **2018**, *272*, 243−251.
(30) Munir, S.; Park, S.-Y. Liquid-Crystal Droplets Functionalized with a Non-Enzymatic Moiety for Glucose Sensing. *Sens. Actuators, B* **2018**, *257*, 579−585.
(31) Myung, D.-b.; Hussain, S.; Park, S.-Y. Photonic Calcium and Humidity Array Sensor Prepared with Reactive Cholesteric Liquid Crystal Mesogens. *Sens. Actuators, B* **2019**, *298*, 126894.
(32) Moirangthem, M.; Arts, R.; Merkx, M.; Schenning, A. P. H. J. An Optical Sensor Based on a Photonic Polymer Film to Detect Calcium in Serum. *Adv. Funct. Mater.* **2016**, *26*, 1154−1160.
(33) Lorand, J. P.; EDWARDS, J. O. Polyol Complexes and Structure of the Benzeneboronate Ion. *J. Org. Chem.* **1959**, *24*, 769−774.

DOI: 10.1021/acsami.9b10316
ACS Appl. Mater. Interfaces 2019, 11, 37434−37441